Original Article

MOLECULAR METABOLISM

Lactate activation of α-cell K_{ATP} channels inhibits glucagon secretion by hyperpolarizing the membrane potential and reducing Ca^{2+} entry

Karolina E. Zaborska [1], Prasanna K. Dadi [1], Matthew T. Dickerson [1], Arya Y. Nakhe [1], Ariel S. Thorson [1], Charles M. Schaub [1], Sarah M. Graff [1], Jade E. Stanley [1], Roy S. Kondapavuluru [1], Jerod S. Denton [2], David A. Jacobson [1,*]

ABSTRACT

Objective: Elevations in pancreatic α-cell intracellular Ca^{2+} ($[Ca^{2+}]_i$) lead to glucagon (GCG) secretion. Although glucose inhibits GCG secretion, how lactate and pyruvate control α-cell Ca^{2+} handling is unknown. Lactate enters cells through monocarboxylate transporters (MCTs) and is also produced during glycolysis by lactate dehydrogenase A (LDHA), an enzyme expressed in α-cells. As lactate activates ATP-sensitive K^+ (K_{ATP}) channels in cardiomyocytes, lactate may also modulate α-cell K_{ATP}. Therefore, this study investigated how lactate signaling controls α-cell Ca^{2+} handling and GCG secretion.

Methods: Mouse and human islets were used in combination with confocal microscopy, electrophysiology, GCG immunoassays, and fluorescent thallium flux assays to assess α-cell Ca^{2+} handling, V_m, K_{ATP} currents, and GCG secretion.

Results: Lactate-inhibited mouse (75 ± 25%) and human (47 ± 9%) α-cell $[Ca^{2+}]_i$ fluctuations only under low-glucose conditions (1 mM) but had no effect on β- or δ-cells $[Ca^{2+}]_i$. Glyburide inhibition of K_{ATP} channels restored α-cell $[Ca^{2+}]_i$ fluctuations in the presence of lactate. Lactate transport into α-cells via MCTs hyperpolarized mouse (14 ± 1 mV) and human (12 ± 1 mV) α-cell V_m and activated K_{ATP} channels. Interestingly, pyruvate showed a similar K_{ATP} activation profile and α-cell $[Ca^{2+}]_i$ inhibition as lactate. Lactate-induced inhibition of α-cell $[Ca^{2+}]_i$ influx resulted in reduced GCG secretion in mouse (62 ± 6%) and human (43 ± 13%) islets.

Conclusions: These data demonstrate for the first time that lactate entry into α-cells through MCTs results in K_{ATP} activation, V_m hyperpolarization, reduced $[Ca^{2+}]_i$, and inhibition of GCG secretion. Thus, taken together, these data indicate that lactate either within α-cells and/or elevated in serum could serve as important modulators of α-cell function.

Keywords α-cells; Ca^{2+} handling; K_{ATP} channels; Glucagon secretion; Lactate; Pyruvate

1. INTRODUCTION

Pancreatic α-cells secrete glucagon (GCG) under low-glucose conditions, which in turn stimulates hepatic glucose output [1—3]. Thus, GCG secretion plays a key role in preventing hypoglycemia and maintaining glucose homeostasis. Ca^{2+} entry into α-cells has been shown to stimulate GCG secretion, and removal of extracellular Ca^{2+} completely inhibits GCG secretion [4,5]. Glucose-regulated electrical excitability controls α-cell Ca^{2+} entry through voltage-dependent Ca^{2+} channels (VDCCs) [6—8], the activity and inactivation of which are tightly controlled by membrane potential (V_m) [9,10]. These glucose-regulated changes in α-cell V_m are regulated by the orchestrated activity of many ion channels. For example, the activity of ATP-sensitive K^+ (K_{ATP}) channels is a critical determinant of α-cell V_m, Ca^{2+} entry and GCG secretion [11,12]. This indicates an important role for V_m modulation of α-cell Ca^{2+} entry and GCG secretion; however, the mechanisms that control α-cell V_m and Ca^{2+} handling remain poorly understood.

Pancreatic α-cells are much more glycolytically active than β-cells; thus, the rate of mitochondrial glucose oxidation in α-cells is 20—40% that of β-cells [13—15]. The increase in glycolytic activity may be due in part to elevated levels of enzymes, such as lactate dehydrogenase (LDH) and pyruvate dehydrogenase kinase 4 in α-cells compared to β-cells; in fact, LDH is only expressed in α-cells and not in β-cells [13—15]. Furthermore, studies on rodent islets cells have observed that LDH activity is increased in non-β-cells, including α-cells [13,16]. Interestingly, glycolytic enzymes or enzymes that metabolize glycolytic products have been shown to interact with and modulate the activity of ion channels. For example, LDH and pyruvate kinase interact with and regulate K_{ATP} channel complexes [17—19]. LDH catalyzes the conversion of pyruvate to lactate, which activates K_{ATP} channels in cardiomyocytes to protect against myocardial ischemia or hypoxia [20].

[1]Department of Molecular Physiology and Biophysics, Vanderbilt University, Nashville, TN 37232, USA [2]Department of Pharmacology, Vanderbilt University, Nashville, TN 37232, USA

*Corresponding author. Department of Molecular Physiology and Biophysics, Vanderbilt University, 7425B MRB IV, 2213 Garland Ave., Nashville, TN, 37232-0615, USA. E-mail: david.a.jacobson@vanderbilt.edu (D.A. Jacobson).

Received July 1, 2020 • Revision received July 17, 2020 • Accepted July 24, 2020 • Available online 28 July 2020

https://doi.org/10.1016/j.molmet.2020.101056

Thus, lactate and pyruvate have been shown to regulate K_{ATP} activity [17–19]. Moreover, other glycolysis products such as 1,3-bisphosphoglycerate also regulate K_{ATP} activity [21,22]. The high expression of LDH in α-cells suggests that it may bind to and modulate K_{ATP} channel function and thus GCG secretion. However, the role of enzymes that regulate the production of glycolytic products or their metabolism have not been assessed for their influence on human α-cell V_m, Ca^{2+} entry, or GCG secretion.

While α-cells metabolize glucose largely via anaerobic glycolysis [13] that produces lactate, lactate is also elevated in cells when serum lactate levels rise or via a lactate shuttle mechanism [23]. For example, blood lactate concentrations are elevated postprandially (up to 1.5–3.7 mM depending on the carbohydrate source) [24–28], which may be an important contributor in controlling glucose inhibition of GCG secretion. Schwann cells also produce and provide lactate for cells that they support [29]. As they are present within and surrounding islets, Schwann cells may influence the local concentration of lactate near α-cells and thus control α-cell function [30,31]. Lactate is transported into cells through monocarboxylate transporters (MCTs), which also transport pyruvate across the plasma membrane [32,33]. Lactate entry was demonstrated to be 3-fold greater in primary α-cells compared to β-cells [16]. As MCTs and LDH are not expressed in β-cells, exogenous lactate has no effect on insulin secretion [16,34]. However, the role of lactate on α-cell function has not been determined.

This study demonstrated for the first time that lactate provides a signal that robustly controls human and mouse α-cell V_m, Ca^{2+} handling, and GCG secretion. Lactate and pyruvate reduced mouse α-cell intracellular Ca^{2+} ($[Ca^{2+}]_i$) under low-glucose conditions but not β- or δ-cell $[Ca^{2+}]_i$. Lactate also reduced human α-cell $[Ca^{2+}]_i$ under low-glucose conditions but had no effect on both human and mouse $[Ca^{2+}]_i$ under high-glucose conditions. Moreover, lactate hyperpolarized mouse and human V_m by activating K_{ATP} channels. These changes induced by lactate or pyruvate decreased mouse and human GCG secretion specifically under low-glucose conditions. These findings highlight the importance of lactate in controlling α-cell $[Ca^{2+}]_i$ and GCG secretion.

2. MATERIALS AND METHODS

2.1. Chemicals and reagents

All of the research materials were purchased from Sigma–Aldrich (St. Louis, MO, USA) or Thermo-Fisher (Waltham, MA, USA) unless otherwise specified. A stable cell line with tetracycline-inducible Kir6.2/SUR1 expression was previously described [35].

2.2. Ethical approval

The animals were handled in compliance with guidelines approved by the Vanderbilt University Animal Care and Use Committee protocols (protocol #M1600063-01). All of the mice used in these studies were 12- to 18-week-old age-matched males with a C57BL/6J background. Transgenic mice expressing a tandem-dimer red fluorescent protein (tdRFP) fluorescent reporter, specifically in α-cells, were generated by crossing mice expressing *GCG*-IRES-Cre with mice expressing a tdRFP fluorescent reporter preceded by a loxP-flanked STOP cassette in the Rosa26 locus (αRFP) [36–38]. Transgenic mice expressing GCaMP3 fluorescent Ca^{2+} indicator, specifically in α-cells, were generated by crossing mice expressing *GCG*-IRES-Cre with mice expressing GCaMP3 preceded by a loxP-flanked STOP cassette in the Rosa26 locus (α-GCaMP3, Stock No. 014538; The Jackson Laboratory) [39]. Similarly, transgenic mice expressing GCaMP6s, specifically in δ-cells, were generated by crossing Sst-IRES-Cre mice (Stock No: 013044; The Jackson Laborator) with mice possessing the genetically encoded Ca^{2+} indicator GCaMP6s preceded by a loxP-flanked STOP cassette (Stock No: 028866; The Jackson Laborato) [40].

Healthy human islets were obtained from multiple isolation centers through the Integrated Islet Distribution Program (IIDP). The IIDP obtained informed consent for deceased donors in accordance with the National Institute of Health guidelines before reception of human islets for our studies. The work detailed herein was approved by the Vanderbilt University Health Sciences Committee Institutional Review Board (IRB# 110164). Human donor information is provided in Supplemental Table 1.

2.3. Pancreas and islet preparation

Mouse pancreata were digested with collagenase P (Roche, Basel, Switzerland) and islets were isolated via density gradient centrifugation as previously described [41–43]. After isolation, mouse islets were either dispersed into islet cell clusters (by titrating in 0.005% trypsin) or maintained as whole islets. They were then plated on poly-D-lysine-coated 35 mm glass-bottomed dishes (CellVis, Mountain View, CA, USA) and cultured in RPMI 1640 medium containing 11 mM glucose and supplemented with 15% fetal bovine serum (FBS), 100 IU·ml^{-1} penicillin, and 100 mg ml^{-1} streptomycin at 37 °C in 5% CO_2.

Human islets were dispersed into single cells by gently titrating in TrypLE Express at 37 °C for 1–2 min. The cells were then incubated with a previously characterized β-cell-specific monoclonal mouse anti-human NTPDase3 antibody [44,45] (5 μg/ml, ectonucleotidases-ab, RRID:AB_2752250; Quebec, Canada) for 30 min at 4 °C followed by 15 min incubation with anti-mouse IgG2a + b magnetic MicroBeads (Miltenyi Biotec, Auburn, CA, USA) at 4 °C. The magnetically labeled β-cells were then separated from the other islet cells (non-β-cells) using an LS column (Miltenyi Biotec). The non-β-cells (containing mainly α-cells) were then either plated on poly-D-lysine-coated 35 mm glass bottom dishes or allowed to re-aggregate in 24-well AggreWell 400 plates (STEMCELL Technologies, Cambridge, MA, USA) at 700–1000 cell density/pseudoislet for 6 days. Human non-β-cells and pseudoislets were cultured in CMRL-1066 (Corning, Cleveland, TN, USA) media containing 5.6 mM glucose and supplemented with 20% FBS, 100 IU·ml^{-1} penicillin, 100 mg ml^{-1} streptomycin, 2 mM GlutaMAX, 2 mM HEPES, and 1 mM sodium pyruvate. Dispersed human islet cells were immunostained to confirm the successful separation of the β-cells from the non-β-cells. The cells were plated on poly-D-lysine-coated 35 mm glass-bottomed dishes and fixed in 4% paraformaldehyde for 20 min. The cells were then stained with primary antibodies (1:100 rat anti-insulin; DSH, Iowa City, IA, USA) and 1:200 mouse anti-glucagon (Abcam, Cambridge, MA, USA) followed by secondary antibodies (1:500 anti-rat Alexa Fluor 488 and 1:500 anti-mouse Alexa Fluor 546). Immunofluorescent images were obtained using a Nikon Ti2 epifluorescence microscope equipped with a Prime 95B camera with 25 mm CMOS sensors and Nikon Elements software.

2.4. Intracellular Ca^{2+} imaging

Intracellular Ca^{2+} ($[Ca^{2+}]_i$) imaging was conducted as previously described using epifluorescent or confocal microscopy with Ca^{2+} dye (Fura-2-acetoxymethyl ester [AM]) [46] or genetic indicators (GCaMP3 or GCaMP6s) [47]. The mouse islets and human non-β-cells were loaded with Fura-2 AM (2 μM) for 25 min at 37 °C in 5% CO_2. The mouse islets and human non-β-cells were incubated in RPMI with either 1 mM or 11 mM glucose for 30 min and then washed and perfused with Krebs–Ringer HEPES buffer containing (mM) 119 NaCl, 10 HEPES, 4.7 KCl, 2 $CaCl_2$, 1.2 $MgSO_4$, and 1.2 KH_2PO_4 (pH 7.35 adjusted by NaOH) with the indicated glucose concentrations and

treatments (see the figure legends). To ensure that osmolarity changes did not influence Ca^{2+} responses, we also conducted experiments confirming lactate inhibition of α-cell Ca^{2+} handling using osmotically balanced solutions (with mannitol; data not shown). The mouse β-cells and human non-β-cells' Fura-2 AM fluorescence was measured at 340 and 380 nm (F_{340}/F_{380}) every 5 s as an indicator of $[Ca^{2+}]_i$ using a Nikon Ti2 microscope. Human α-cells were identified from the non-β-cells by perfusing them with epinephrine (20 μM) at the end of each protocol as previously described to increase $[Ca^{2+}]_i$ specifically in α-cells [48]. Mouse α-cell GCaMP3 and δ-cell GCaMP6s fluorescence was measured at 488 nm every 5 s as an indicator of $[Ca^{2+}]_i$ using a Zeiss Observer Z1 confocal microscope equipped with a Yokogawa CSU-X1 spinning disk head and PerkinElmer Volocity software (Zeiss spinning disk) or a Nikon Ti2 microscope. As GCaMP3 and GCaMP6s are single wavelength Ca^{2+} probes, all of the data were normalized to the minimum fluorescence intensity at 488 nm (F/F_{min}).

2.5. Measurement of cytosolic lactate, Ad Laconic

Mouse αRFP islet cell clusters were transduced with a genetically encoded Forster resonance energy transfer (FRET) lactate sensor (Laconic; Addgene, Watertown, MA, USA) in an adenoviral format (Ad Laconic; $5*10^6$ PFU) in RPMI for 4 h at 37 °C in 5% CO_2 as previously described [49]. The cell clusters were imaged 24 h after incubation with Ad Laconic using a Nikon Ti2 epifluorescence microscope. The cell clusters were excited at 430 nm and the fluorescence emission intensity of mTFP and Venus were measured every 5 s at 485 nm and 528 nm, respectively. The ratio between the emission wavelengths of mTFP and Venus were used to quantify the intracellular concentration of lactate within the cells. Transduced mouse α-cells were identified by tdRFP fluorescence.

2.6. Thallium flux assay

Thallium (Tl^+) flux assays were conducted as previously described [50]. Briefly, stably transfected T-REx-HEK-293 cells expressing $K_{ir}6.2$/SUR1 (K_{ATP}) channels were cultured overnight in Dulbecco's Modified Eagle's Medium supplemented with 1% GlutaMAX, 10% FBS, and 1 μg/ml tetracycline at 37 °C in 5% CO_2. The cells were washed with assay buffer (Hanks' balanced salt solution with 20 mM HEPES and pH 7.3) and then loaded with Tl^+-sensitive dye (Thallos-AM, 2 μM) for 1 h at 37 °C. Plates were washed with assay buffer and a baseline recording was collected at 1 Hz for 10 s (excitation 470 ± 20 nm and emission 540 ± 30 nm) using a Panoptic whole-plate kinetic imager (Wavefront Biosciences, Franklin, TN, USA). Lactate was then added (7-point concentration curve; 0.05 mM—10 mM) and dissolved in assay buffer containing K_{ATP} activator (VU0071063, 7 μM) for a 5-minute incubation period while continuing data collection. Tl^+ stimulus buffer (5x in mM: 125 D-gluconic acid sodium salt, 7.5 Tl_2SO_4, 1 $MgSO_4$, 1.8 $CaSO_4$, 5 D-glucose, 20 HEPES, and pH 7.3) was added and data were collected for an additional 3 min. The data were then analyzed using GraphPad Prism.

2.7. Patch-clamp electrophysiology

For K_{ATP} current recordings, αRFP mouse islets were dispersed into single cells by titrating in 0.005% trypsin and cultured overnight in RMPI supplemented with 11 mM glucose at 37 °C in 5% CO2. Patch electrodes (3—4 MΩ) employed for K_{ATP} current recordings were backfilled with intracellular solution containing (in mM) 140 KCl, 0.5 MgCl2, 10 EGTA, 0.1 Mg-ATP, and 5 HEPES (pH 7.25 adjusted with KOH). RFP-positive mouse α-cells were patched in extracellular solution (EC) containing (in mM) 140 NaCl, 3.6 KCl, 0.5 $MgSO_4$, 1.5 $CaCl_2$, 0.5 NaH_2PO_4, 5 $NaHCO_3$, and 10 HEPES (pH 7.35 with NaOH) supplemented with 1 mM glucose and treatments as indicated in the figure legends, with sucrose added as needed to match the osmolarity. Whole-cell currents were measured as a function of the applied membrane voltage (voltage ramp from −120 to 60 mV) in voltage-clamp mode using an Axopatch 200B amplifier with pCLAMP10 software (Molecular Devices, San Jose, CA, USA) every 15 s starting immediately after a whole-cell configuration was established between patch pipettes and α-cells as previously described [43,46,50]. This recording protocol was repeated until the whole-cell currents reached a plateau that corresponded to the maximum K_{ATP} current activation. K_{ATP} currents stimulated by reducing intracellular ATP (0.1 mM) were calculated by subtracting the initial current traces from the maximum current traces.

For V_m recordings, αRFP mouse islets were partially dispersed into islet cell clusters (20—50 cells) by titrating in 0.005% trypsin and cultured overnight in RPMI supplemented with 11 mM glucose at 37 °C in 5% CO_2; human α-cell pseudoislets were cultured overnight in CMRL-1066 supplemented with 5.6 mM glucose. Patch electrodes utilized for V_m recordings were backfilled with intracellular solution containing (in mM) 10 KCl, 76 K_2SO_4, 1 $MgCl_2$, and 5 HEPES (pH 7.25 with KOH) supplemented with 0.4 mg/L of gramicidin perforating reagent. RFP-positive mouse α-cells and human α-cells were patched in EC supplemented with 1 mM glucose. After a perforated-patch configuration was established, the V_m of the α-cells within the αRFP mouse islet cell clusters or human α-cell pseudoislets was recorded in current-clamp mode. The electrical activity of the patched α-cells was recorded for at least 10 min under these conditions; the patched α-cells were then stimulated with treatments as indicated in the figure legends.

2.8. Glucagon secretion

The mouse and human islets were allowed to recover for 24 h after isolation and 4 h after reception, respectively, in RPMI 1640 supplemented with 15% FBS, 11 mM glucose (5.6 mM for human islets), and 0.5 mg/ml BSA at 37 °C in 5% CO_2. GCG secretion measurements from static incubations were conducted as previously described [39]. GCG concentrations were determined by a Vanderbilt Hormone Assay and Analytical Services Core using a GCG radioimmunoassay kit or GCG Chemiluminescence ELISA (ALPCO; Salem, NH, USA) under the conditions indicated in the figure legends.

2.9. Statistical analyses

All of the data are presented as mean ± standard error (SE) for the specified number of samples (*N*). The statistical analysis was conducted using GraphPad Prism 8 with two-tailed t-tests or one-way ANOVA as appropriate. $P < 0.05$ was considered statistically significant.

3. RESULTS

3.1. Lactate reduces mouse and human α-cell $[Ca^{2+}]_i$

Although lactate is an important energy source, nothing is known about how it regulates α-cell function. Therefore, we tested whether lactate regulates α-cell Ca^{2+} handling and if this is due to paracrine signaling from β- or δ-cells. This was accomplished in intact mouse islets using genetically encoded Ca^{2+} indicator GCaMP expressed specifically in either α- or δ-cells, while β-cell $[Ca^{2+}]_i$ was monitored using a Ca^{2+} dye (Fura-2 AM). Lactate (10 mM) significantly decreased $[Ca^{2+}]_i$ in the mouse α-cells under low-glucose conditions (1 mM) (75 ± 25% decrease, $P < 0.05$, $N = 8$, Figure 1A,C) but not in the β- ($N = 3$, Figure 1G,I) or δ-cells ($N = 3$, Figure 1D,F). Under high-glucose

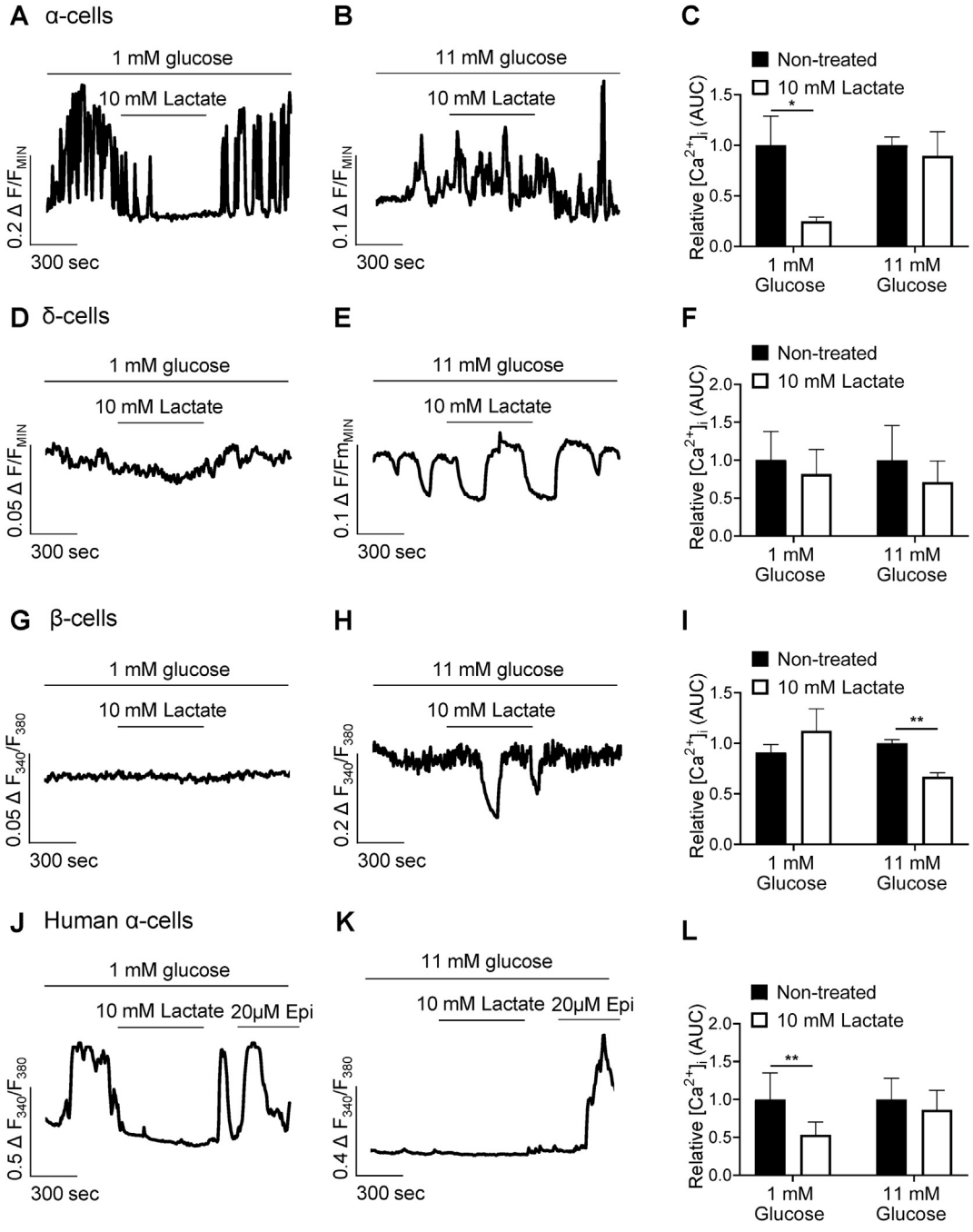

Figure 1: Lactate reduces α-cell $[Ca^{2+}]_i$. Representative α-cell GCaMP3 recording (A and B) and relative fluorescence AUC (C) at 1 mM and 11 mM glucose in whole mouse islets in the presence or absence of 10 mM lactate. Representative δ-cell GCaMP6 recording (D and E) and relative fluorescence AUC (F) at 1 mM and 11 mM glucose in whole mouse islets in the presence or absence of 10 mM lactate. Representative Fura-2 AM recording from β-cells (G and H) and relative fluorescence AUC (I) at 1 mM and 11 mM glucose in whole mouse islets in the presence or absence of 10 mM lactate. Representative α-cell Fura-2AM recording (J and K) and relative fluorescence AUC (L) at 1 mM and 11 mM glucose in dispersed human α-cells in the presence or absence of 10 mM lactate. $N = 3$–8. The statistical analysis was conducted using the two-tailed unpaired Student's t-test, and uncertainty is expressed as SE (*$P < 0.05$ and **$P < 0.01$).

conditions (11 mM), lactate transiently reduced β-cell $[Ca^{2+}]_i$ (33 ± 1% decrease, $P < 0.01$, $N = 3$, Figure 1H,I) but did not impact α- ($N = 3$, Figure 1B,C) or δ-cells ($N = 3$, Figure 1E,F) $[Ca^{2+}]_i$. Moreover, the physiological plasma levels of lactate (2 mM) also attenuated α-cell $[Ca^{2+}]_i$ under low-glucose conditions (1 mM) (58 ± 12% decrease, $P < 0.05$, $N = 4$, Figure S1). These data demonstrate that lactate significantly attenuated mouse α-cell $[Ca^{2+}]_i$ specifically under low-glucose conditions and transiently reduced β-cell $[Ca^{2+}]_i$ under high-glucose conditions.

We next determined whether lactate transport into and/or metabolism in α-cells plays a role in modulating Ca^{2+} handling. L-lactate is the principal isomer produced by humans, while D-lactate is the predominant isomer produced by some bacterial species [51,52]. The only α-cell LDH that can convert lactate into pyruvate is LDHA

[53], which is selective for L-lactate. Therefore, we investigated the effects of D-lactate on mouse α-cell $[Ca^{2+}]_i$. Interestingly, D-lactate (10 mM) had no effect on mouse α-cell $[Ca^{2+}]_i$ under low-glucose conditions (1 mM) ($N = 3$, Figure S2). This suggests that either LDHA is involved in the inhibition of α-cell Ca^{2+} influx or that L-lactate metabolism generates a signal that is required to limit α-cell Ca^{2+} influx.

We then determined whether lactate also regulates human α-cell $[Ca^{2+}]_i$. This was achieved by imaging $[Ca^{2+}]_i$ in the human α-cells that were dispersed and magnetically separated from the β-cells. To confirm the successful separation of the β-cells from the non-β-cells, we immunostained for insulin and glucagon. Most of the cells in the non-β-cell fraction were glucagon-positive cells (Figure S3), indicating the successful separation of the β-cells from the non-β-cells. To confirm that the imaged cells were α-cells, we exposed the cells to epinephrine (20 μM) at the end of the imaging protocol and only the cells that showed an increase in $[Ca^{2+}]_i$ were considered α-cells [48]. Lactate (10 mM) significantly reduced $[Ca^{2+}]_i$ in the human α-cells under low-glucose conditions (1 mM) (47 ± 9% decrease, $P < 0.01$, $N = 4$, Figure 1J,K) but had no effect under high-glucose conditions (11 mM) ($N = 3$, Figure 1K and L), highlighting the importance of lactate as a modulator of human α-cell $[Ca^{2+}]_i$.

3.2. Pyruvate attenuates mouse α-cell $[Ca^{2+}]_i$

LDHA is known to catalyze the conversion of pyruvate into lactate; therefore, we investigated whether pyruvate mimics the effects of lactate on α-cell Ca^{2+} entry. Pyruvate (10 mM) also attenuated α-cell $[Ca^{2+}]_i$ under low-glucose conditions (1 mM; 34 ± 13% decrease, $N = 3$, $P < 0.05$, Figure 2A,C) but not under high-glucose conditions (11 mM; $N = 3$, Figure 2B,C). Pyruvate had no effect on β- ($N = 3$, Figure 2G,I) or δ-cells ($N = 3$, Figure 2D,F) under low-glucose conditions (1 mM), but pyruvate transiently decreased β-cell $[Ca^{2+}]_i$ under high-glucose conditions (11 mM) (29 ± 1% decrease, $N = 3$, $P < 0.001$, Figure 2H,I). This may suggest that α-cell glycolytic production of pyruvate reduces Ca^{2+} and GCG secretion. As glucose inhibits GCG secretion with a U-shaped concentration response, elevations of glucose levels above 11 mM begin to lose inhibitory tone on GCG secretion. Interestingly, we found that glucose inhibition of

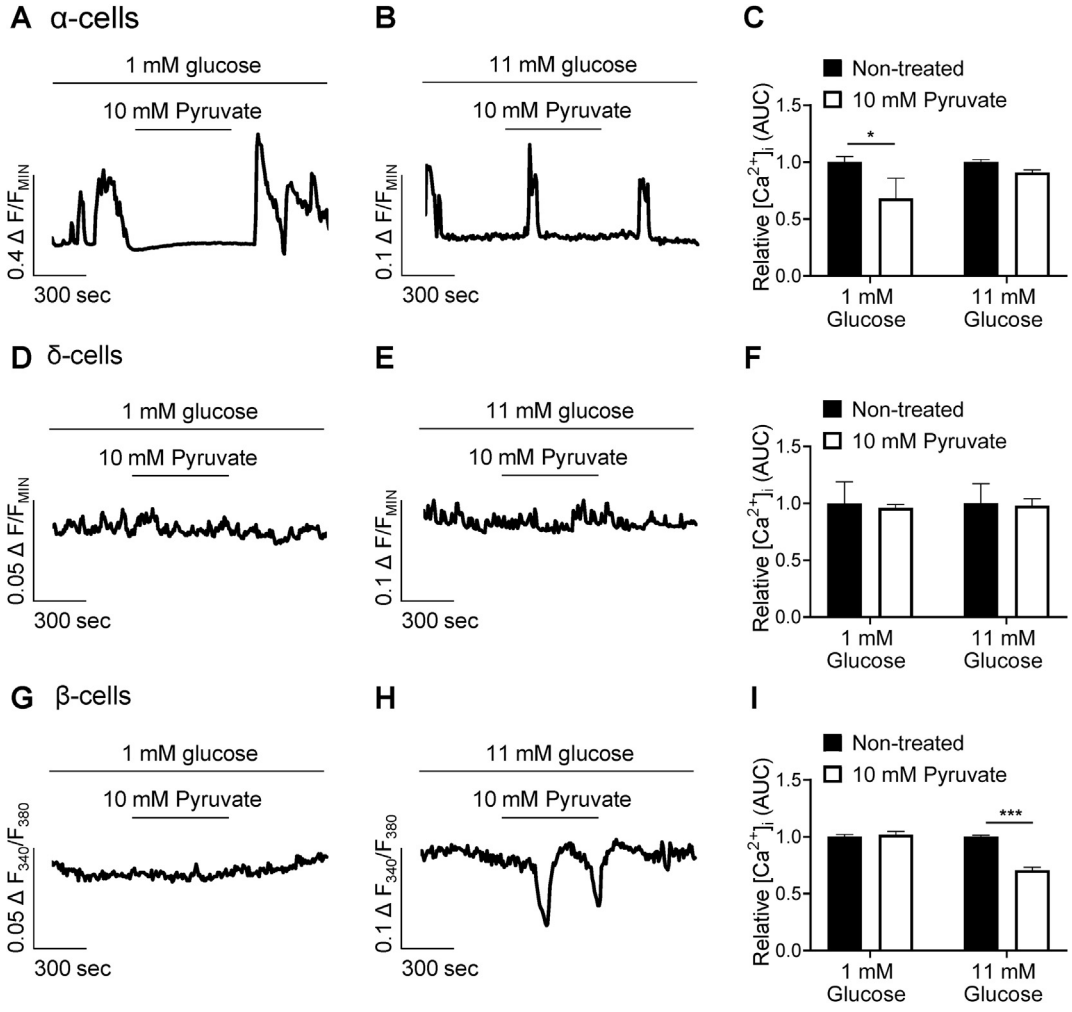

Figure 2: Pyruvate decreases α-cell $[Ca^{2+}]_i$. Representative α-cell GCaMP3 recording (A and B) and relative fluorescence AUC (C) at 1 mM and 11 mM glucose in whole mouse islets in the presence or absence of 10 mM pyruvate. Representative δ-cell GCaMP6 recording (D and E) and relative fluorescence AUC (F) at 1 mM and 11 mM glucose in whole mouse islets in the presence or absence of 10 mM pyruvate. Representative Fura-2 AM recording from β-cells (G and H) and relative fluorescence AUC (I) at 1 mM and 11 mM glucose in whole mouse islets in the presence or absence of 10 mM pyruvate. $N = 3$. The statistical analysis was conducted using the two-tailed unpaired Student's t-test, and uncertainty is expressed as SE (*$P < 0.05$ and ***$P < 0.001$).

pyruvate activity on α-cell Ca^{2+} was lost under 20 mM glucose conditions, and pyruvate was still able to inhibit Ca^{2+} influx (62 ± 14% decrease, $N = 3$, $P < 0.05$, Figure S4A and B). These data show that pyruvate attenuates mouse α-cell $[Ca^{2+}]_i$ only under glucose conditions when GCG secretion occurs.

3.3. Monocarboxylate transporters transport lactate into mouse α-cells

Lactate is known to enter the cells through MCTs [32,33] and activate the $G\alpha_{i/o}$-coupled receptor GPR81 [54,55]; therefore, we wanted to establish whether lactate transport into α-cells is required for its effect on $[Ca^{2+}]_i$. Using the Laconic intracellular lactate sensor, we found that treatment with exogenous lactate resulted in its transport into α-cells (Figure 3A,B, $N = 3$, $P < 0.0001$). To determine if GPR81 is involved in lactate response, we activated GPR81 with a selective agonist (3Cl-HBA, 50 μM) and found no effect on α-cell $[Ca^{2+}]_i$ ($N = 3$, Figure S5A and B). To confirm this, we incubated islets with pertussis toxin (1 μg/ml for 24 h) to inhibit $G\alpha_{i/o}$ signaling. Under these conditions, lactate was still able to reduce α-cell $[Ca^{2+}]_i$ ($N = 3$, Figure S5C and D, $P < 0.05$). We next assessed whether lactate transport through MCTs is required for lactate-induced reduction in α-cell $[Ca^{2+}]_i$. In the presence of MCT1/2/4 inhibitor (BAY8002, 2 μM), lactate inhibition of islet α-cell $[Ca^{2+}]_i$ under low-glucose conditions (1 mM) was abolished ($N = 3$, Figure 3C–F). However, as the MCT1 inhibitor (7ACC2, 100 nM) did not impact the lactate inhibition of α-cell $[Ca^{2+}]_i$, MCT1 was not required for the lactate effect. Taken together, these data demonstrate that lactate transport through MCTs (presumably MCT2 and/or MCT4) is necessary for lactate entry into α-cells and the resulting inhibition of Ca^{2+} influx.

3.4. Lactate hyperpolarizes mouse and human α-cells

To investigate the mechanism(s) by which lactate transport controls α-cell $[Ca^{2+}]_i$, we assessed if VDCC activity could be impacted by changes in V_m. Treatment with lactate resulted in hyperpolarization of mouse (14 ± 1 mV hyperpolarization, $N = 3$, $P < 0.05$, Figure 4A,B) and human (12 ± 1 mV hyperpolarization, $N = 3$, $P < 0.01$, Figure 4D,E, and G) α-cell V_m. This resulted in either slowing or inhibition of action potential firing in both mouse (1.9 ± 0.4 Hz decrease, $P < 0.05$, $N = 3$, Figure 4C) and human (0.4 ± 0.1 Hz decrease, $N = 3$, Figure 4F; $P < 0.05$) α-cells. These data suggest that lactate activates a hyperpolarizing conductance in α-cells, which is predicted to limit VDCC activity and reduce Ca^{2+} influx.

To determine if K^+ channels such as K_{ATP} contribute to lactate-induced V_m hyperpolarization, we first clamped α-cell Ca^{2+} with a constant V_m depolarization by shifting the reversal potential through K^+ channels with high (30 mM) K^+ and K_{ATP} activator diazoxide (200 μM). Under these conditions, lactate had no effect on α-cell $[Ca^{2+}]_i$ ($N = 3$, Figure 4H,I). This suggests that a K^+ channel is likely responsible for lactate-induced hyperpolarization.

3.5. Lactate and pyruvate activate K_{ATP} channels in α-cells

To determine the ion channels involved in lactate-induced inhibition of α-cell $[Ca^{2+}]_i$, we utilized pharmacology and ion substitution. First, we tested Cl^- channels by imaging the response of mouse α-cells to lactate in Cl^--free solution and found that lactate was still able to reduce α-cell $[Ca^{2+}]_i$ (59 ± 3% decrease, $P < 0.01$, $N = 3$, Figure 5A,B) in the absence of Cl^- flux. Next, we investigated the contributions of large conductance calcium-activated K^+ channels (BK) and G protein-coupled inwardly rectifying K^+ channels (GIRK) to the lactate effect on α-cell $[Ca^{2+}]_i$ using the BK channel inhibitor

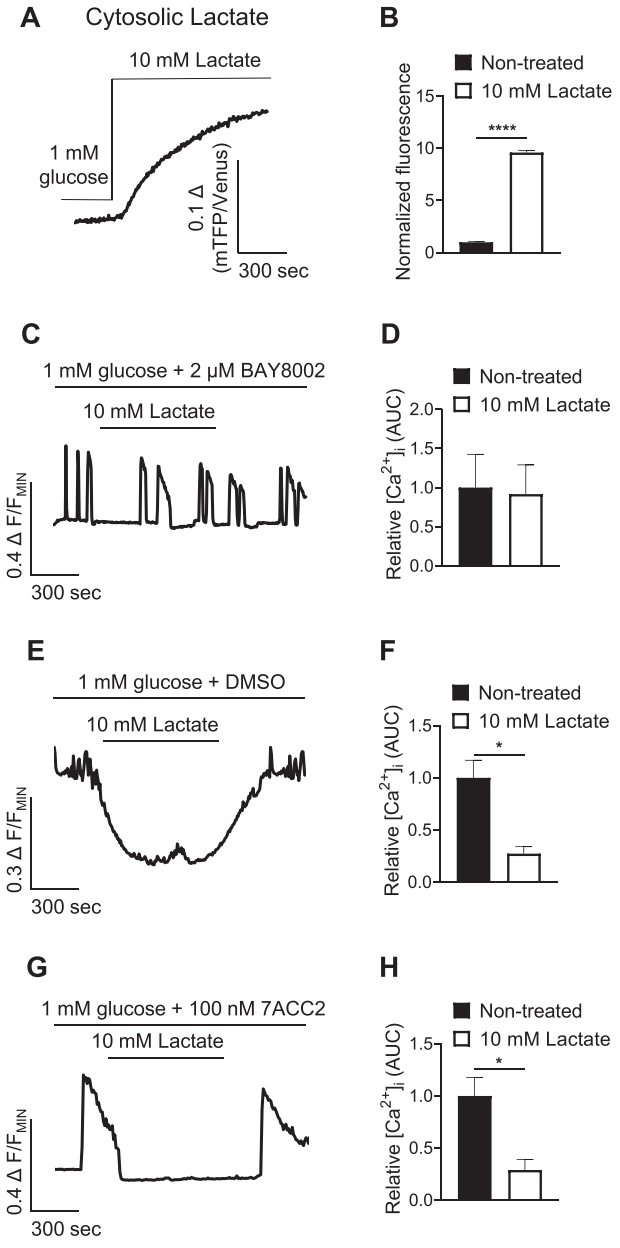

Figure 3: Lactate entry into α-cell via monocarboxylate transporters reduces $[Ca^{2+}]_i$. Representative lactate entry recording (A) and relative fluorescence AUC (B) from dispersed red fluorescent protein-expressing (αRFP) α-cells in 1 mM glucose before and after the addition of 10 mM lactate. Representative α-cell GCaMP3 recording (C) and relative fluorescence AUC (D) at 1 mM glucose in whole islets in the presence or absence of 10 mM lactate continuously treated with a MCT1/2/4 inhibitor (2 μM BAY8002) or vehicle control (E,F). Representative α-cell GCaMP3 recording (G) and relative fluorescence AUC (H) at 1 mM glucose in whole islets in the presence or absence of 10 mM lactate continuously treated with a MCT1 inhibitor (100 nM 7ACC2). $N = 3$. The statistical analysis was conducted using the two-tailed unpaired Student's t-test, and uncertainty is expressed as SE (*$P < 0.05$ and ****$P < 0.0001$).

(Iberiotoxin, 100 nM) and a GIRK channel blocker (Tertiapin-Q, 100 nM). Lactate retained its ability to reduce α-cell $[Ca^{2+}]_i$ in the presence of Iberiotoxin and Tertiapin-Q (BK: 73 ± 13%, $P < 0.05$, $N = 3$, Figure 5C,D; GIRK: 70 ± 14%, $N = 3$, $P < 0.05$, Figure 5E,F). We also investigated the role of K_{ATP} channels and found that during lactate treatment, the addition of the K_{ATP} channel inhibitor glyburide (100 μM) attenuated the lactate-induced reduction of α-cell $[Ca^{2+}]_i$

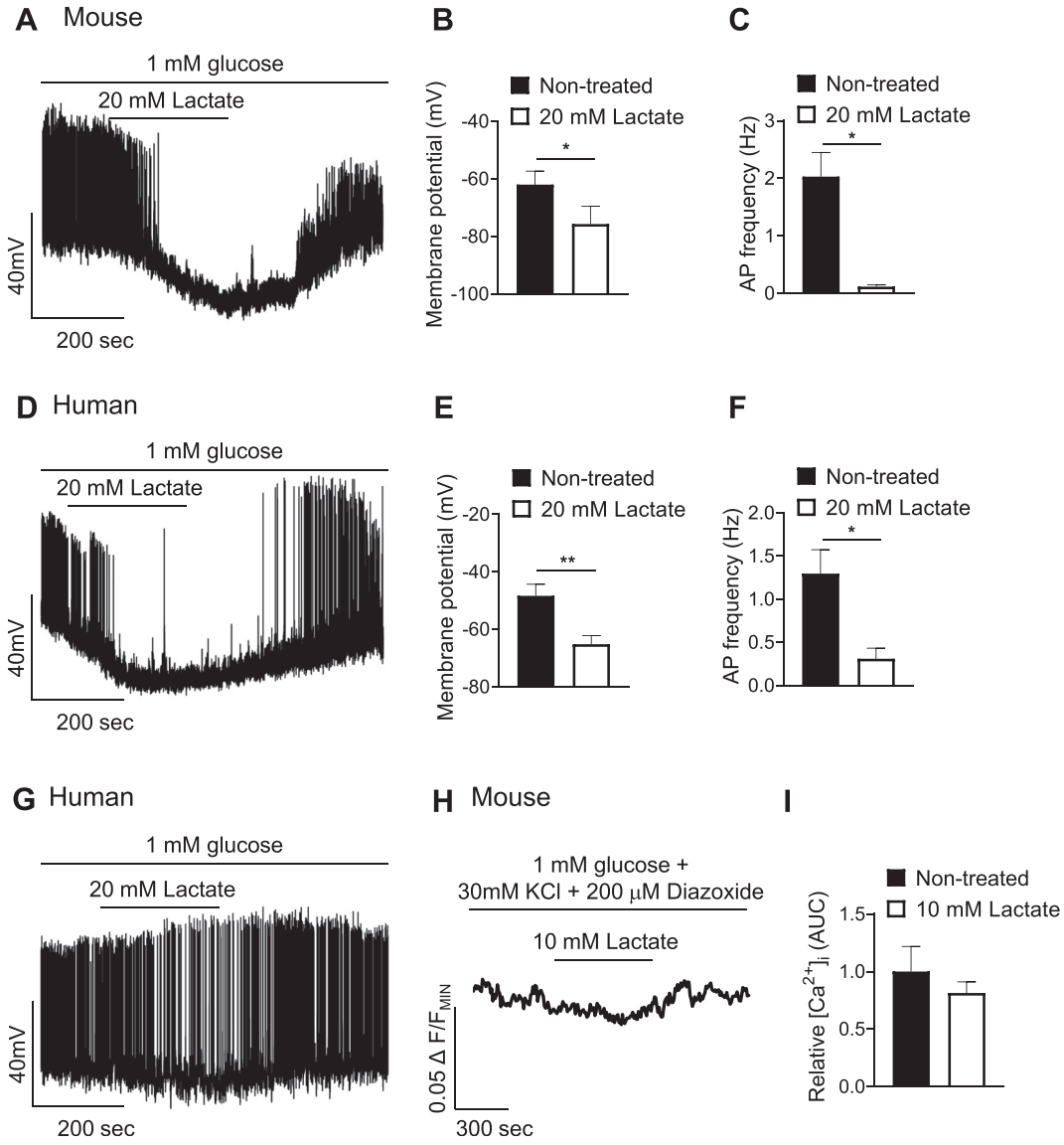

Figure 4: Lactate hyperpolarizes α-cells. Representative membrane potential (V_m) recording (A) and average V_m (B) from dispersed fluorescent protein-expressing (αRFP) α-cells at 1 mM glucose in whole mouse islets ($N = 3$ cells/3 mice) before and after the addition of 20 mM lactate. Representative membrane potential (V_m) recordings (D and G) and average V_m (E) from α-cells at 1 mM glucose in human non-β-cells pseudoislets ($N = 6$ cells/3 islet donors) before and after the addition of 20 mM lactate. Average action potential frequency from αRFP α-cells at 1 mM glucose in whole mouse islets ($N = 3$ cells/3 mice; C) and human non-β-cell pseudoislets ($N = 6$ cells/3 islet donors; F) before and after the addition of 20 mM lactate. Representative α-cell GCaMP3 recording (H) and relative fluorescence AUC (I) at 1 mM glucose in whole islets in the presence or absence of 10 mM lactate continuously treated with 30 mM KCl and 200 μM diazoxide ($N = 3$ mice). The statistical analysis was conducted using the two-tailed unpaired Student's t-test, and uncertainty is expressed as SE (*$P < 0.05$ and **$P < 0.01$).

($N = 3$, $P < 0.01$, Figure 5G,H). This suggested that K_{ATP} is responsible for the lactate-induced V_m hyperpolarization and the resulting reduction of $[Ca^{2+}]_i$.

To test if lactate and pyruvate activate K_{ATP} channels, we measured K_{ATP} currents and used a fluorescent Tl^+ flux readout for K_{ATP} channel activity [50]. Using a 7-point concentration curve (0.05 mM–10 mM), we determined that Tl^+ flux through K_{ATP} channels was activated by both lactate ($N = 3$, Figure 6A,B; EC_{50}: 1.8 mM ± 95% confidence interval [95% CI]: 0.69–5.4 mM) and pyruvate ($N = 3$, Figure 6C,D; EC_{50}: 1.9 mM±[95% CI]: 1.4–3.4 mM). Lactate and pyruvate can activate K_{ATP} channels in the presence of low glucose (Figure S6A and B) or with a pharmacological K_{ATP} activator (7 μM; Figure 6A–D). We next measured K_{ATP} currents in mouse α-cells and found that the K_{ATP} current density was significantly increased in α-cells in response to lactate ($N = 4$, Figure 6E,F, $P < 0.01$) and pyruvate ($N = 4$, Figure 6G,H, $P < 0.001$). Taken together, these data demonstrate that lactate and pyruvate activate K_{ATP} channels in mouse α-cells, which mediates the lactate-induced reduction of α-cell $[Ca^{2+}]_i$.

3.6. Lactate and pyruvate reduce GCG secretion

As Ca^{2+} entry into α-cells stimulates GCG secretion [4,5], we next investigated the effects of lactate and pyruvate on GCG secretion in human and mouse islets. Lactate significantly reduced GCG secretion in both the mouse (62 ± 6% decrease, $P < 0.05$, $N = 3$, Figure 7A) and human (43 ± 13% decrease, $N = 5$, $P < 0.01$, Figure 7B) islets

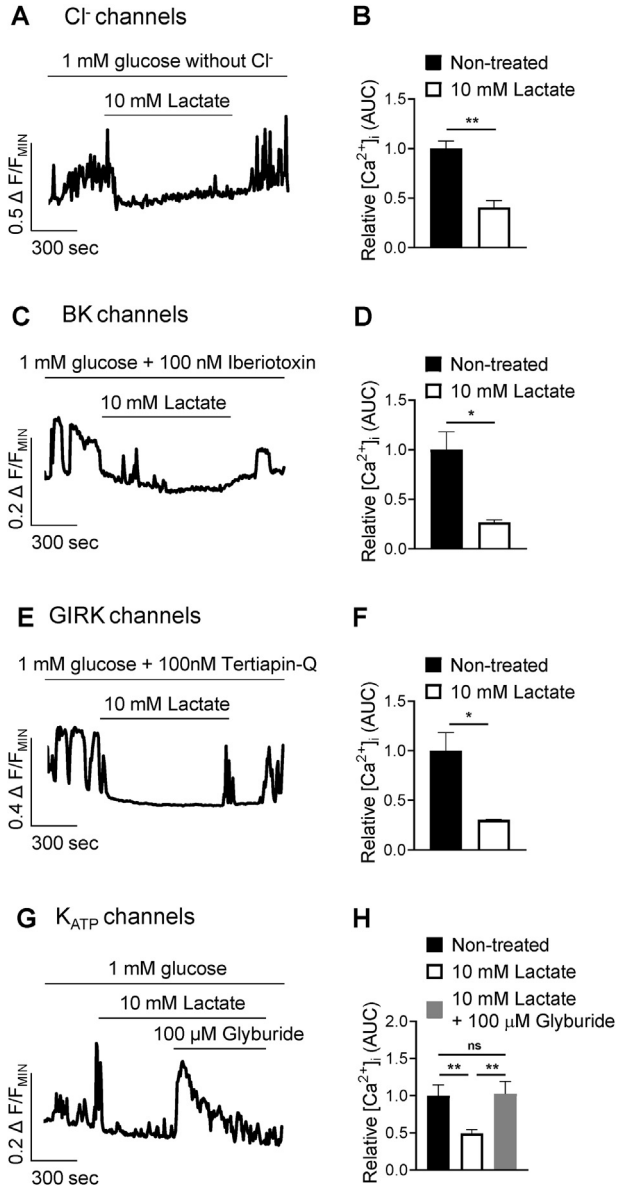

Figure 5: Lactate reduces α-cell $[Ca^{2+}]_i$ through activation of K_{ATP} channels. Representative α-cell GCaMP3 recording (A) and relative fluorescence AUC (B) at 1 mM glucose (without Cl^-) in whole islets in the presence or absence of 10 mM lactate. Representative α-cell GCaMP3 recording and relative fluorescence AUC at 1 mM glucose in whole islets in the presence or absence of 10 mM lactate continuously treated with a BK channel inhibitor (100 nM Iberiotoxin; C and D) or GIRK channel inhibitor (100 nM Tertiapin-Q; E and F). Representative α-cell GCaMP3 recording (G) and relative fluorescence AUC (H) at 1 mM glucose in whole islets in the presence or absence of 10 mM lactate or K_{ATP} channel blocker (100 μM glyburide). $N = 3$ mice. The statistical analysis was conducted using two-tailed unpaired Student's t-test, and uncertainty is expressed as SE (*$P < 0.05$ and **$P < 0.01$).

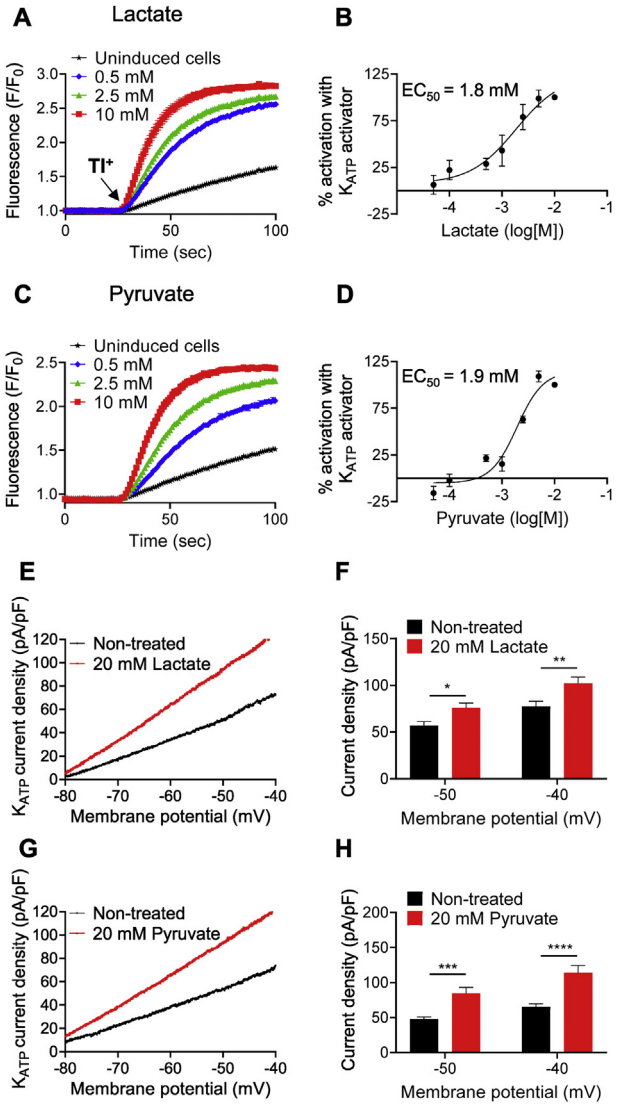

Figure 6: Lactate and pyruvate activate K_{ATP} channels. Representative thallium (Tl^+) flux recordings from T-REx-HEK-293 cells expressing K_{ATP} channels treated with lactate (A; $N = 3$) or pyruvate (C; $N = 3$) (0.5, 2.5, and 10 mM) and uninduced K_{ATP} cells. Fluorescence values were normalized (F/F_0) to baseline values recorded before Tl^+ addition. Dose-dependent activation of K_{ATP} by lactate (B; $N = 3$) or pyruvate (D; $N = 3$). Area under the curve data are expressed as % activation calculated as % change in K_{ATP} activation by lactate or pyruvate compared to K_{ATP} activation by vehicle control (assay buffer with 7 μM K_{ATP} activator). Estimated EC_{50} values were calculated using 3-parameter (lactate) or 4-parameter (pyruvate) logistic regression fit. Representative K_{ATP} current recorded from dispersed red fluorescent protein-expressing (αRFP) α-cells in the presence or absence of 20 mM lactate (E) or 20 mM pyruvate (G). Average K_{ATP} currents ($N \geq 28$ cells/4 mice) from α-cells in the presence or absence of 20 mM lactate (F) or 20 mM pyruvate (H). The statistical analysis was conducted using the unpaired two-tailed Student's t-test, and uncertainty is expressed as SE (*$P < 0.05$, **$P < 0.01$, ***$P < 0.001$, and ****$P < 0.0001$).

under low-glucose conditions (1 mM) but had no effect under high-glucose conditions (11 mM). Similarly, pyruvate reduced GCG secretion under low-glucose conditions (1 mM) in the mouse (62 ± 11% decrease, $N = 3$, $P < 0.01$, Figure 7C) and human (37 ± 3% decrease, $N = 3$, $P < 0.01$, Figure 7D) islets but not under high-glucose conditions (11 mM). These responses follow the glucose-sensitive changes in α-cell Ca^{2+} handling observed in response to lactate and pyruvate. These data indicate that lactate and pyruvate inhibition of α-cell $[Ca^{2+}]_i$ limits GCG secretion.

4. DISCUSSION

Secretion of islet GCG plays a key role in maintaining blood glucose homeostasis; however, our understanding of α-cell function remains poorly understood. It has been established that Ca^{2+} entry is required for GCG secretion but the factor(s) that modulate α-cell Ca^{2+} handling are still largely unknown. In this study, we demonstrated for the first time that lactate signaling plays a key role in regulating both human

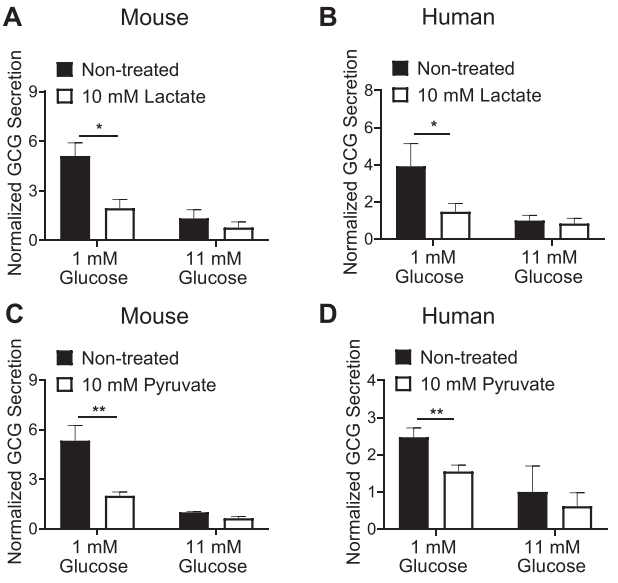

Figure 7: Lactate and pyruvate reduce islet glucagon secretion. Average GCG secretion from mouse (A) and human (B) islets treated with or without 10 mM lactate at 1 mM (mouse $N = 3$; human $N = 5$) and 11 mM glucose (mouse $N = 6$; human $N = 5$) normalized to the total islet number and 11 mM glucose. (B) Average GCG secretion from mouse (C) and human (D) islets treated with or without 10 mM pyruvate at 1 mM and 11 mM glucose normalized to the total islet number and 11 mM glucose ($N = 3$). The statistical analysis was conducted using the two-tailed unpaired Student's t-test, and uncertainty is expressed as SE ($^*P < 0.05$ and $^{**}P < 0.01$).

and mouse α-cell V_m, Ca^{2+} handling, and GCG secretion. We found that lactate and pyruvate reduced α-cell $[Ca^{2+}]_i$ under low-glucose conditions and that lactate entry into α-cells through MCTs is required for the inhibition of $[Ca^{2+}]_i$. Moreover, lactate hyperpolarized both mouse and human α-cell V_m by activating K_{ATP} channels. Lactate and pyruvate activation of K_{ATP} channels inhibited Ca^{2+} entry and resulted in inhibition of GCG secretion from both mouse and human islets. Taken together, these data suggest that lactate is a critical regulator of α-cell Ca^{2+} handling and GCG secretion.

Pancreatic α-cell Ca^{2+} handling and GCG secretion is controlled by metabolism; however, the influence of lactate and pyruvate on α-cell Ca^{2+} handling have not been determined. Lactate plays important roles in controlling Ca^{2+} handling in other tissues; for example, lactate inhibits Ca^{2+} entry into the myometrium [56]. Lactate-induced inhibition of Ca^{2+} entry into the myometrium is abolished by depolarization with KCl, suggesting that myometrial K^+ channels are activated by lactate; this is similar to our findings demonstrating that lactate reduces α-cell $[Ca^{2+}]_i$ through α-cell V_m hyperpolarization by K_{ATP} activation. Moreover, lactate causes intracellular acidification in the myometrium, similar to lactate-induced acidification of rat islet non-β-cells (presumably α-cells) [16]. High glucose also results in α-cell acidification [57], which contributes to glucose inhibition of GCG secretion. As proton movement during lactate transport through MCTs causes intracellular acidification [58], lactate-induced α-cell proton flux could contribute to reducing GCG secretion. Low levels of MCT expression in β-cells do not allow significant lactate transport or pH changes in response to elevations in extracellular lactate [16]. The reduced rate of lactate transport likely contributes to the lack of effect of lactate on β- and δ-cell $[Ca^{2+}]_i$ under low-glucose conditions and only transient effects on β-cell $[Ca^{2+}]_i$ under high-glucose conditions. However, the transient reduction in β-cell $[Ca^{2+}]_i$ had no effects on α-cell $[Ca^{2+}]_i$ under high-glucose conditions. Interestingly, pyruvate exerted similar inhibitory effects on mouse pancreatic α-cell $[Ca^{2+}]_i$ and GCG secretion as lactate, which differed from previous data obtained from perfused rat pancreas showing that pyruvate increases GCG secretion [34]. This discrepancy could be explained by species differences as well as different experimental conditions (different glucose concentrations and secretion measurements). These findings on rat islets were suggested to be due to metabolic activation of GCG secretion by pyruvate entry into α-cells through MCT and a lack of effect of pyruvate on other islet cells due to a lack of MCT expression. Our findings also suggest that lactate and pyruvate enter α-cells through MCTs but are further in line with data showing that metabolic factors such as glucose can intrinsically impart inhibitory tone on α-cell GCG secretion [59]. Our data provide novel details on pyruvate and lactate control of α-cell function through inhibition of cytoplasmic Ca^{2+} handling, which illuminate mechanistic insights into how metabolic intermediates can impact GCG secretion.

It has been well established that α-cell Ca^{2+} entry through VDCCs is tightly coupled to changes in V_m. The α-cell V_m is controlled by ion channels, such as K_{ATP} channels, voltage-gated K^+ (Kv) channels, G protein-coupled inwardly rectifying K^+ (GIRK) channels, and two-pore domain K^+ (K2P) channels [6,9,10,12,39,40,60,61]. Inhibition of K^+ channels can result in reduced GCG secretion due to depolarization-induced voltage-dependent inactivation of VDCCs as well as voltage-dependent Na^+ channels [8,11,12,61]. However, hyperpolarization has also been shown to inhibit α-cell VDCC activity during glucose stimulation [6,39,62–66]. Furthermore, somatostatin (SST) signaling-induced activation of GIRK channels hyperpolarizes α-cell V_m to inhibit GCG secretion [67]. Our findings with lactate treatment also support that hyperpolarization of α-cell V_m limits GCG secretion by reducing VDCC activity. The importance of lactate and pyruvate-mediated V_m hyperpolarization is exemplified in hepatocytes, where it increases activity of K^+ channels and potentially Na^+/K^+ ATPase [68]. While this suggests that lactate has intrinsic effect(s) on V_m, paracrine signals (such as SST) are known to hyperpolarize α-cell V_m [67]. However, our data demonstrating that single α-cells exhibit lactate-mediated inhibition of $[Ca^{2+}]_i$ indicates an intrinsic V_m hyperpolarizing mechanism. Furthermore, lactate does not impact β-cell insulin secretion [16,34] and is not predicted to impact SST secretion as there is no response of δ-cell $[Ca^{2+}]_i$ to lactate. Inhibition of Gi signaling had no impact on lactate-induced inhibition of α-cell $[Ca^{2+}]_i$. Taken together, this suggests that lactate entry into α-cells activates a K^+ channel leading to V_m hyperpolarization, which ultimately inhibits Ca^{2+} entry and GCG secretion.

One of the critical K^+ channel regulators of α-cell V_m is the ATP-sensitive K_{ATP} channel. As lactate and pyruvate are known to be metabolized and increase ATP production, K_{ATP} activity is likely modulated by lactate and pyruvate. Indeed, we found that inhibition of K_{ATP} channels abolished the lactate-induced reduction in α-cell $[Ca^{2+}]_i$. This is an interesting finding as lactate and pyruvate-mediated increases in ATP are predicted to close K_{ATP} channels and depolarize α-cell V_m. However, glucose-induced ATP production in α-cells is significantly lower than in β-cells [34,69] and the ATP/ADP ratio is much higher in α-cells compared to β-cells under low-glucose conditions [15]. This is due to metabolic differences observed between β- and α-cells (α-cells are more glycolytic active and do not produce as much ATP due to lower oxidative phosphorylation). Even if lactate and pyruvate were to increase α-cell ATP levels, then this would be predicted to inhibit K_{ATP} channels. Thus, this suggests that lactate and pyruvate control of ATP levels does not lead to inactivation of K_{ATP}. While it has been proposed that the ATP/ADP ratio is the primary regulator of K_{ATP}, there are other mechanisms that control K_{ATP} that

have not been assessed in α-cells. For example, pyruvate and lactate allosterically activate cardiomyocyte K_{ATP} channel complexes with lactate dehydrogenase [17]. This is consistent with our findings showing that lactate and pyruvate activate α-cell K_{ATP} channels. Although LDH control of K_{ATP} is a likely candidate for the lactate-mediated reduction in α-cell $[Ca^{2+}]_i$, pH can also regulate K_{ATP} activity [70]. As pyruvate and lactate movement across MCTs causes intracellular acidification and K_{ATP} is inhibited by acidification, the changes in pH by lactate or pyruvate likely do not activate K_{ATP} channels. This is further supported by our studies clamping intracellular pyruvate and lactate under physiological pH levels that both resulted in increased K_{ATP} activity. This suggests the exciting possibility that glycolysis might also contribute to activation of α-cell K_{ATP} channels through LDHA. This is supported by data showing that inhibition of K_{ATP} under euglycemic glucose conditions leads to stimulation of GCG secretion [71]. However, pharmacological inhibition of whole islet K_{ATP} channels also causes significant increases in insulin and SST secretion under euglycemic conditions, which may explain why other groups have observed sulfonylurea inhibition of GCG secretion [72,73]. How glucose production of lactate and pyruvate contributes to glucose inhibition of GCG secretion remains to be determined; however, our results suggest that ATP is not the only signal that α-cells utilize to control K_{ATP} conductance and thus GCG secretion.

Lactate is a major source of energy and can have autocrine-, paracrine-, and endocrine-like effects. Importantly, during postprandial elevations of blood glucose, its metabolism leads to an increase in blood lactate and pyruvate levels [24—28]. The carbohydrate type plays an important role in the postprandial increase in lactate and pyruvate concentrations, with high-sucrose [26] and high-fructose [25] meals leading to greater lactate and pyruvate levels than high-starch or high-glucose meals, respectively. While this suggests that elevations in blood lactate and pyruvate could play a role in postprandial inhibition of GCG secretion, plasma pyruvate levels do not reach more than 1 mM, which does not activate K_{ATP} or influence α-cell Ca^{2+} handling. However, lactate levels range from 1.5 to 3.7 mM postprandially, which is at or above the EC_{50} for K_{ATP} activation and also reduces α-cell $[Ca^{2+}]_i$. Therefore, the combined elevations in glucose and lactate could help reduce GCG secretion postprandially. Interestingly, insulin resistance in T2D leads to increased blood lactate levels [74—78] due to mitochondrial dysfunction and hypoxic conditions [79—81]. Furthermore, due to increased basal plasma lactate levels, the postprandial change in lactate following a meal is significantly reduced in T2D. Thus, this reduction in meal-induced lactate response may contribute to postprandial hyperglucagonemia in T2D patients [82] due to reduced lactate inhibition of GCG secretion. GCG signaling also increases hepatic lactate output [83] and thus in T2D, elevated GCG levels may contribute to increased lactate levels. It has become clear that there is a bidirectional communication between the liver and α-cells that impacts GCG secretion and α-cell hyperplasia. For example, reduced liver GCG signaling results in increased hepatic amino acid output that increases α-cell proliferation and GCG secretion [84]. Therefore, increased hepatic lactate output during elevated GCG signaling might serve to reduce GCG secretion and potentially α-cell proliferation. Taken together, our findings illuminate that alterations in lactate levels may serve an important signaling role in GCG secretion. Furthermore, insulin resistance-induced perturbations in lactate homeostasis could be involved in dysfunctional GCG secretion.

In conclusion, our data indicate that lactate plays a key role in regulating α-cell Ca^{2+} handling and GCG secretion. This suggests the exciting possibility that lactate and pyruvate and/or enzymes in the pathway play an important role in controlling α-cell function. As exogenous lactate is only able to exert its effects under conditions that stimulate GCG secretion, this suggests that either intrinsic lactate may play a role in glucose inhibition of GCG secretion or that exogenous lactate can only inhibit secretagogue-stimulated Ca^{2+} entry. While we also observed that pyruvate inhibits α-cell Ca^{2+} handling and GCG secretion, the pyruvate concentration used in our studies significantly exceeded circulating pyruvate levels; this indicates that fluctuations in serum pyruvate do not play a role in modulating α-cell function. However, circulating postprandial lactate levels reach concentrations ($\geq$1.5 mM) that activate K_{ATP} channels, which may play a role in modulating GCG secretion. Importantly, the postprandial increase in blood lactate levels is diminished in T2D; thus, reduced lactate inhibition of GCG secretion may contribute to hyperglucagonemia in T2D patients. Overall, these observations improve our understanding of the molecular mechanisms regulating α-cell V_m, $[Ca^{2+}]_i$, and GCG secretion.

AUTHOR CONTRIBUTIONS

DAJ and KEZ conceived the project. KEZ, PKD, MTD, AYN, AST, CMS, SMG, JES, and RSK conducted the experiments and analyzed the data. JSD created the K_{ATP} cell line, provided valuable expertise, and edited the manuscript. KEZ and DAJ wrote and edited the manuscript.

ACKNOWLEDGMENTS

This study was conducted with the support of the Integrated Islet Distribution Program (IIDP; https://iidp.coh.org/). We would especially like to thank the organ donors and their families. This project was funded by the Juvenile Diabetes Research Foundation (grant: 2-SRA-2019-701-S-B). In addition, this research was supported by the National Institutes of Health (NIH grant: DK097392) and The Leona M. and Harry B. Helmsley Charitable Trust (grant: 602987). The glucagon immunoassays were carried out by the Vanderbilt Hormone Assay Core (supported by NIH grants: DK059637 and DK020593). We would like to thank Dr. Alvin C. Powers and Dr. Diane C. Saunders for providing the β-cell-specific monoclonal mouse anti-human NTPDase3 antibody. Confocal microscopy was conducted using the Vanderbilt Cell Imaging Shared Resource (NIH grant: DK020593).

CONFLICT OF INTEREST

The authors declare no conflicts of interest.

APPENDIX A. SUPPLEMENTARY DATA

Supplementary data to this article can be found online at https://doi.org/10.1016/j.molmet.2020.101056.

REFERENCES

[1] König, M., Bulik, S., Holzhütter, H.-G., 2012. Quantifying the contribution of the liver to glucose homeostasis: a detailed kinetic model of human hepatic glucose metabolism. PLoS Computational Biology 8(6):e1002577.

[2] Miller, R.A., Birnbaum, M.J., 2016. Glucagon: acute actions on hepatic metabolism. Diabetologia 59(7):1376—1381.

[3] Ramnanan, C., Edgerton, D., Kraft, G., Cherrington, A., 2011. Physiologic action of glucagon on liver glucose metabolism. Diabetes, Obesity and Metabolism 13(s1):118—125.

[4] Gerich, J.E., Frankel, B.J., Fanska, R., West, L., Forsham, P.H., Grodsky, G.M., 1974. Calcium dependency of glucagon secretion from the in vitro perfused rat pancreas. Endocrinology 94(5):1381—1385.

[5] Lundquist, I., Fanska, R., Grodsky, G.M., 1976. Interaction of calcium and glucose on glucagon secretion. Endocrinology 99(5):1304—1312.

[6] MacDonald, P.E., De Marinis, Y.Z., Ramracheya, R., Salehi, A., Ma, X., Johnson, P.R., et al., 2007. A KATP channel-dependent pathway within α cells regulates glucagon release from both rodent and human islets of Langerhans. PLoS Biology 5(6):e143.

[7] Munoz, A., Hu, M., Hussain, K., Bryan, J., Aguilar-Bryan, L., Rajan, A.S., 2005. Regulation of glucagon secretion at low glucose concentrations: evidence for adenosine triphosphate-sensitive potassium channel involvement. Endocrinology 146(12):5514—5521.

[8] Ramracheya, R., Ward, C., Shigeto, M., Walker, J.N., Amisten, S., Zhang, Q., et al., 2010. Membrane potential-dependent inactivation of voltage-gated ion channels in α-cells inhibits glucagon secretion from human islets. Diabetes 59(9):2198—2208.

[9] Catterall, W.A., 2011. Voltage-gated calcium channels. Cold Spring Harbor Perspectives in Biology 3(8):a003947.

[10] Snutch, T.P., Peloquin, J., Mathews, E., McRory, J.E., 2005. Molecular Properties of Voltage-Gated Calcium Channels. Voltage-Gated Calcium Channels. Springer. p. 61—94.

[11] Gopel, S.O., Kanno, T., Barg, S., Weng, X.G., Gromada, J., Rorsman, P., 2000. Regulation of glucagon release in mouse -cells by KATP channels and inactivation of TTX-sensitive Na+ channels. Journal of Physiology 528(Pt 3):509—520.

[12] Zhang, Q., Ramracheya, R., Lahmann, C., Tarasov, A., Bengtsson, M., Braha, O., et al., 2013. Role of KATP channels in glucose-regulated glucagon secretion and impaired counterregulation in type 2 diabetes. Cell Metabolism 18(6):871—882.

[13] Schuit, F., De Vos, A., Farfari, S., Moens, K., Pipeleers, D., Brun, T., et al., 1997. Metabolic fate of glucose in purified islet cells. Glucose-regulated anaplerosis in beta cells. Journal of Biological Chemistry 272(30):18572—18579.

[14] Gorus, F.K., Malaisse, W.J., Pipeleers, D.G., 1984. Differences in glucose handling by pancreatic A- and B-cells. Journal of Biological Chemistry 259(2):1196—1200.

[15] Detimary, P., Dejonghe, S., Ling, Z., Pipeleers, D., Schuit, F., Henquin, J.C., 1998. The changes in adenine nucleotides measured in glucose-stimulated rodent islets occur in beta cells but not in alpha cells and are also observed in human islets. Journal of Biological Chemistry 273(51):33905—33908.

[16] Sekine, N., Cirulli, V., Regazzi, R., Brown, L.J., Gine, E., Tamarit-Rodriguez, J., et al., 1994. Low lactate dehydrogenase and high mitochondrial glycerol phosphate dehydrogenase in pancreatic beta-cells. Potential role in nutrient sensing. Journal of Biological Chemistry 269(7):4895—4902.

[17] Crawford, R.M., Budas, G.R., Jovanovic, S., Ranki, H.J., Wilson, T.J., Davies, A.M., et al., 2002. M-LDH serves as a sarcolemmal K(ATP) channel subunit essential for cell protection against ischemia. The EMBO Journal 21(15):3936—3948.

[18] Hong, M., Kefaloyianni, E., Bao, L., Malester, B., Delaroche, D., Neubert, T.A., et al., 2011. Cardiac ATP-sensitive K+ channel associates with the glycolytic enzyme complex. The FASEB Journal 25(7):2456—2467.

[19] Dhar-Chowdhury, P., Harrell, M.D., Han, S.Y., Jankowska, D., Parachuru, L., Morrissey, A., et al., 2005. The glycolytic enzymes, glyceraldehyde-3-phosphate dehydrogenase, triose-phosphate isomerase, and pyruvate kinase are components of the K(ATP) channel macromolecular complex and regulate its function. Journal of Biological Chemistry 280(46):38464—38470.

[20] Han, J., So, I., Kim, E.Y., Earm, Y.E., 1993. ATP-sensitive potassium channels are modulated by intracellular lactate in rabbit ventricular myocytes. Pflügers Archiv 425(5—6):546—548.

[21] Jovanovic, S., Du, Q., Crawford, R.M., Budas, G.R., Stagljar, I., Jovanovic, A., 2005. Glyceraldehyde 3-phosphate dehydrogenase serves as an accessory protein of the cardiac sarcolemmal K(ATP) channel. EMBO Reports 6(9):848—852.

[22] Jovanovic, S., Jovanovic, A., 2005. High glucose regulates the activity of cardiac sarcolemmal ATP-sensitive K+ channels via 1,3-bisphosphoglycerate: a novel link between cardiac membrane excitability and glucose metabolism. Diabetes 54(2):383—393.

[23] Brooks, G.A., 2002. Lactate shuttles in nature. Biochemical Society Transactions 30(2):258—264.

[24] Berhane, F., Fite, A., Daboul, N., Al-Janabi, W., Msallaty, Z., Caruso, M., et al., 2015. Plasma lactate levels increase during hyperinsulinemic euglycemic clamp and oral glucose tolerance test. Journal of Diabetes Research 2015:102054.

[25] Brundin, T., Wahren, J., 1993. Whole body and splanchnic oxygen consumption and blood flow after oral ingestion of fructose or glucose. American Journal of Physiology 264(4 Pt 1):E504—E513.

[26] Daly, M.E., Vale, C., Walker, M., Littlefield, A., George, K., Alberti, M., et al., 2000. Acute fuel selection in response to high-sucrose and high-starch meals in healthy men. American Journal of Clinical Nutrition 71(6):1516—1524.

[27] Doar, J.W., Cramp, D.G., Maw, D.S., Seed, M., Wynn, V., 1970. Blood pyruvate and lactate levels during oral and intravenous glucose tolerance tests in diabetes mellitus. Clinical Science 39(2):259—269.

[28] Reaven, G.M., Hollenbeck, C., Jeng, C.Y., Wu, M.S., Chen, Y.D., 1988. Measurement of plasma glucose, free fatty acid, lactate, and insulin for 24 h in patients with NIDDM. Diabetes 37(8):1020—1024.

[29] Brown, A.M., Evans, R.D., Black, J., Ransom, B.R., 2012. Schwann cell glycogen selectively supports myelinated axon function. Annals of Neurology 72(3):406—418.

[30] Donev, S.R., 1984. Ultrastructural evidence for the presence of a glial sheath investing the islets of Langerhans in the pancreas of mammals. Cell and Tissue Research 237(2):343—348.

[31] Sunami, E., Kanazawa, H., Hashizume, H., Takeda, M., Hatakeyama, K., Ushiki, T., 2001. Morphological characteristics of Schwann cells in the islets of Langerhans of the murine pancreas. Archives of Histology & Cytology 64(2):191—201.

[32] Garcia, C.K., Goldstein, J.L., Pathak, R.K., Anderson, R.G., Brown, M.S., 1994. Molecular characterization of a membrane transporter for lactate, pyruvate, and other monocarboxylates: implications for the Cori cycle. Cell 76(5):865—873.

[33] Halestrap, A.P., 2013. The SLC16 gene family - structure, role and regulation in health and disease. Molecular Aspects of Medicine 34(2—3):337—349.

[34] Ishihara, H., Maechler, P., Gjinovci, A., Herrera, P.L., Wollheim, C.B., 2003. Islet beta-cell secretion determines glucagon release from neighbouring alpha-cells. Nature Cell Biology 5(4):330—335.

[35] Raphemot, R., Swale, D.R., Dadi, P.K., Jacobson, D.A., Cooper, P., Wojtovich, A.P., et al., 2014. Direct activation of beta-cell KATP channels with a novel xanthine derivative. Molecular Pharmacology 85(6):858—865.

[36] Herrera, P.L., 2000. Adult insulin- and glucagon-producing cells differentiate from two independent cell lineages. Development 127(11):2317—2322.

[37] Le Marchand, S.J., Piston, D.W., 2010. Glucose suppression of glucagon secretion: metabolic and calcium responses from alpha-cells in intact mouse pancreatic islets. Journal of Biological Chemistry 285(19):14389—14398.

[38] Luche, H., Weber, O., Nageswara Rao, T., Blum, C., Fehling, H.J., 2007. Faithful activation of an extra-bright red fluorescent protein in "knock-in" Cre-reporter mice ideally suited for lineage tracing studies. European Journal of Immunology 37(1):43—53.

[39] Dadi, P.K., Luo, B., Vierra, N.C., Jacobson, D.A., 2015. TASK-1 potassium channels limit pancreatic alpha-cell calcium influx and glucagon secretion. Molecular Endocrinology 29(5):777—787.

[40] Vierra, N.C., Dickerson, M.T., Jordan, K.L., Dadi, P.K., Kadare, K.A., Altman, M.K., et al., 2018. TALK-1 reduces delta-cell endoplasmic reticulum and cytoplasmic calcium levels limiting somatostatin secretion. Molecular Metabolism.

[41] Dickerson, M.T., Bogart, A.M., Altman, M.K., Milian, S.C., Jordan, K.L., Dadi, P.K., et al., 2018. Cytokine-mediated changes in K^+ channel activity promotes an adaptive Ca^{2+} response that sustains β-cell insulin secretion during inflammation. Scientific Reports 8(1):1158.

[42] Dickerson, M.T., Vierra, N.C., Milian, S.C., Dadi, P.K., Jacobson, D.A., 2017. Osteopontin activates the diabetes-associated potassium channel TALK-1 in pancreatic β-cells. PloS One 12(4):e0175069.

[43] Vierra, N.C., Dadi, P.K., Jeong, I., Dickerson, M., Powell, D.R., Jacobson, D.A., 2015. The type-2 diabetes-associated K^+ channel TALK-1 modulates beta-cell electrical excitability, 2nd-phase insulin secretion, and glucose homeostasis. Diabetes, db150280.

[44] Munkonda, M.N., Pelletier, J., Ivanenkov, V.V., Fausther, M., Tremblay, A., Kunzli, B., et al., 2009. Characterization of a monoclonal antibody as the first specific inhibitor of human NTP diphosphohydrolase-3 : partial characterization of the inhibitory epitope and potential applications. FEBS Journal 276(2):479—496.

[45] Saunders, D.C., Brissova, M., Phillips, N., Shrestha, S., Walker, J.T., Aramandla, R., et al., 2019. Ectonucleoside triphosphate diphosphohydrolase-3 antibody targets adult human pancreatic beta cells for in vitro and in vivo analysis. Cell Metabolism 29(3):745—754 e744.

[46] Dickerson, M.T., Dadi, P.K., Altman, M.K., Verlage, K.R., Thorson, A.S., Jordan, K.L., et al., 2019. Glucose-mediated inhibition of calcium-activated potassium channels limits alpha-cell calcium influx and glucagon secretion. American Journal of Physiology Endocrinology and Metabolism 316(4):E646—E659.

[47] Vierra, N.C., Dadi, P.K., Milian, S.C., Dickerson, M.T., Jordan, K.L., Gilon, P., et al., 2017. TALK-1 channels control β cell endoplasmic reticulum Ca^{2+} homeostasis. Science Signaling 10(497):eaan2883.

[48] Hamilton, A., Zhang, Q., Salehi, A., Willems, M., Knudsen, J.G., Ringgaard, A.K., et al., 2018. Adrenaline stimulates glucagon secretion by tpc2-dependent Ca(2+) mobilization from acidic stores in pancreatic alpha-cells. Diabetes 67(6):1128—1139.

[49] San Martin, A., Ceballo, S., Ruminot, I., Lerchundi, R., Frommer, W.B., Barros, L.F., 2013. A genetically encoded FRET lactate sensor and its use to detect the Warburg effect in single cancer cells. PloS One 8(2):e57712.

[50] Dadi, P.K., Vierra, N.C., Days, E., Dickerson, M.T., Vinson, P.N., Weaver, C.D., et al., 2017. Selective small molecule activators of TREK-2 channels stimulate dorsal root ganglion c-fiber nociceptor two-pore-domain potassium channel currents and limit calcium influx. ACS Chemical Neuroscience 8(3):558—568.

[51] Adeva-Andany, M., Lopez-Ojen, M., Funcasta-Calderon, R., Ameneiros-Rodriguez, E., Donapetry-Garcia, C., Vila-Altesor, M., et al., 2014. Comprehensive review on lactate metabolism in human health. Mitochondrion 17:76—100.

[52] Connor, H., Woods, H.F., Ledingham, J.G., 1983. Comparison of the kinetics and utilisation of D(-)-and L(+)-sodium lactate in normal man. Annals of Nutrition & Metabolism 27(6):481—487.

[53] Talasniemi, J.P., Pennanen, S., Savolainen, H., Niskanen, L., Liesivuori, J., 2008. Analytical investigation: assay of D-lactate in diabetic plasma and urine. Clinical Biochemistry 41(13):1099—1103.

[54] Ahmed, K., Tunaru, S., Tang, C., Muller, M., Gille, A., Sassmann, A., et al., 2010. An autocrine lactate loop mediates insulin-dependent inhibition of lipolysis through GPR81. Cell Metabolism 11(4):311—319.

[55] Liu, C., Wu, J., Zhu, J., Kuei, C., Yu, J., Shelton, J., et al., 2009. Lactate inhibits lipolysis in fat cells through activation of an orphan G-protein-coupled receptor, GPR81. Journal of Biological Chemistry 284(5):2811—2822.

[56] Hanley, J.A., Weeks, A., Wray, S., 2015. Physiological increases in lactate inhibit intracellular calcium transients, acidify myocytes and decrease force in term pregnant rat myometrium. Journal of Physiology 593(20):4603—4614.

[57] Knudsen, J.G., Hamilton, A., Ramracheya, R., Tarasov, A.I., Brereton, M., Haythorne, E., et al., 2019. Dysregulation of glucagon secretion by hyperglycemia-induced sodium-dependent reduction of ATP production. Cell Metabolism 29(2):430—442 e434.

[58] Juel, C., Halestrap, A.P., 1999. Lactate transport in skeletal muscle - role and regulation of the monocarboxylate transporter. Journal of Physiology 517(Pt 3):633—642.

[59] Basco, D., Zhang, Q., Salehi, A., Tarasov, A., Dolci, W., Herrera, P., et al., 2018. α-cell glucokinase suppresses glucose-regulated glucagon secretion. Nature Communications 9(1):546.

[60] Kailey, B., van de Bunt, M., Cheley, S., Johnson, P.R., MacDonald, P.E., Gloyn, A.L., et al., 2012. SSTR2 is the functionally dominant somatostatin receptor in human pancreatic beta- and alpha-cells. American Journal of Physiology Endocrinology and Metabolism 303(9):E1107—E1116.

[61] Spigelman, A., Dai, X., MacDonald, P., 2010. Voltage-dependent K^+ channels are positive regulators of alpha cell action potential generation and glucagon secretion in mice and humans. Diabetologia 53(9):1917—1926.

[62] Manning Fox, J.E., Gyulkhandanyan, A.V., Satin, L.S., Wheeler, M.B., 2006. Oscillatory membrane potential response to glucose in islet beta-cells: a comparison of islet-cell electrical activity in mouse and rat. Endocrinology 147(10):4655—4663.

[63] Allister, E.M., Robson-Doucette, C.A., Prentice, K.J., Hardy, A.B., Sultan, S., Gaisano, H.Y., et al., 2013. UCP2 regulates the glucagon response to fasting and starvation. Diabetes 62(5):1623—1633.

[64] Bokvist, K., Olsen, H.L., Hoy, M., Gotfredsen, C.F., Holmes, W.F., Buschard, K., et al., 1999. Characterisation of sulphonylurea and ATP-regulated K+ channels in rat pancreatic A-cells. Pflügers Archiv 438(4):428—436.

[65] Quoix, N., Cheng-Xue, R., Mattart, L., Zeinoun, Z., Guiot, Y., Beauvois, M.C., et al., 2009. Glucose and pharmacological modulators of ATP-sensitive K+ channels control [Ca2+]c by different mechanisms in isolated mouse alpha-cells. Diabetes 58(2):412—421.

[66] Rorsman, P., Salehi, S.A., Abdulkader, F., Braun, M., MacDonald, P.E., 2008. K(ATP)-channels and glucose-regulated glucagon secretion. Trends in Endocrinology and Metabolism 19(8):277—284.

[67] Briant, L., Salehi, A., Vergari, E., Zhang, Q., Rorsman, P., 2016. Glucagon secretion from pancreatic α-cells. Upsala Journal of Medical Sciences 121(2):113—119.

[68] Lutz, T.A., Wild, S., Boutellier, S., Sutter, D., Volkert, M., Scharrer, E., 1998. Hyperpolarization of the cell membrane of mouse hepatocytes by lactate, pyruvate, and fructose is due to Ca2+-dependent activation of K+ channels and of the Na+/K+-ATPase. Biochimica et Biophysica Acta 1372(2):359—369.

[69] Ravier, M.A., Rutter, G.A., 2005. Glucose or insulin, but not zinc ions, inhibit glucagon secretion from mouse pancreatic alpha-cells. Diabetes 54(6):1789—1797.

[70] Baukrowitz, T., Tucker, S.J., Schulte, U., Benndorf, K., Ruppersberg, J.P., Fakler, B., 1999. Inward rectification in KATP channels: a pH switch in the pore. The EMBO Journal 18(4):847—853.

[71] Cheng-Xue, R., Gómez-Ruiz, A., Antoine, N., Noël, L.A., Chae, H.-Y., Ravier, M.A., et al., 2013. Tolbutamide controls glucagon release from mouse islets differently than glucose: involvement of KATP channels from both α-cells and δ-cells. Diabetes 62(5):1612—1622.

[72] Ostenson, C.G., Nylen, A., Grill, V., Gutniak, M., Efendic, S., 1986. Sulfonylurea-induced inhibition of glucagon secretion from the perfused rat pancreas: evidence for a direct, non-paracrine effect. Diabetologia 29(12):861—867.

[73] Ashcroft, F.M., Rorsman, P., 2013. K(ATP) channels and islet hormone secretion: new insights and controversies. Nature Reviews Endocrinology 9(11):660—669.

[74] Chen, Y.D., Varasteh, B.B., Reaven, G.M., 1993. Plasma lactate concentration in obesity and type 2 diabetes. Diabete & Metabolisme 19(4):348—354.

[75] Del Prato, S., Bonadonna, R.C., Bonora, E., Gulli, G., Solini, A., Shank, M., et al., 1993. Characterization of cellular defects of insulin action in type 2 (non-

insulin-dependent) diabetes mellitus. Journal of Clinical Investigation 91(2): 484–494.

[76] Meyer, C., Stumvoll, M., Nadkarni, V., Dostou, J., Mitrakou, A., Gerich, J., 1998. Abnormal renal and hepatic glucose metabolism in type 2 diabetes mellitus. Journal of Clinical Investigation 102(3):619–624.

[77] van der Merwe, M.T., Schlaphoff, G.P., Crowther, N.J., Boyd, I.H., Gray, I.P., Joffe, B.I., et al., 2001. Lactate and glycerol release from adipose tissue in lean, obese, and diabetic women from South Africa. Journal of Clinical Endocrinology & Metabolism 86(7):3296–3303.

[78] Woerle, H.J., Szoke, E., Meyer, C., Dostou, J.M., Wittlin, S.D., Gosmanov, N.R., et al., 2006. Mechanisms for abnormal postprandial glucose metabolism in type 2 diabetes. American Journal of Physiology Endocrinology and Metabolism 290(1):E67–E77.

[79] Gerbitz, K.D., Gempel, K., Brdiczka, D., 1996. Mitochondria and diabetes. Genetic, biochemical, and clinical implications of the cellular energy circuit. Diabetes 45(2):113–126.

[80] Lowell, B.B., Shulman, G.I., 2005. Mitochondrial dysfunction and type 2 diabetes. Science 307(5708):384–387.

[81] Simoneau, J.A., Colberg, S.R., Thaete, F.L., Kelley, D.E., 1995. Skeletal muscle glycolytic and oxidative enzyme capacities are determinants of insulin sensitivity and muscle composition in obese women. The FASEB Journal 9(2):273–278.

[82] Aleksandar, J., Vladan, P., Markovic-Jovanovic, S., Stolic, R., Mitic, J., Smilic, T., 2016. Hyperlactatemia and the outcome of type 2 diabetic patients suffering acute myocardial infarction. Journal of Diabetes Research 2016:6901345.

[83] Davis, M.A., Williams, P.E., Cherrington, A.D., 1985. Effect of glucagon on hepatic lactate metabolism in the conscious dog. American Journal of Physiology 248(4 Pt 1):E463–E470.

[84] Janah, L., Kjeldsen, S., Galsgaard, K.D., Winther-Sorensen, M., Stojanovska, E., Pedersen, J., et al., 2019. Glucagon receptor signaling and glucagon resistance. International Journal of Molecular Sciences 20(13).

